https://doi.org/10.3311/PPci.21896

Periodica Polytechnica Civil Engineering, 68(1), pp. 289–304, 2024

Finite Element Analyses of Cast-in-situ RC Flat Slab with an Equivalent Frame for Horizontal Loads

Zsolt Roszevák[1*], István Haris[1]

[1] Department of Structural Engineering, Faculty of Civil Engineering, Budapest University of Technologies and Economics, Műegyetem rkp. 3., H-1111 Budapest, Hungary
[*] Corresponding author, e-mail: roszevak.zsolt@emk.bme.hu

Received: 19 January 2023, Accepted: 13 September 2023, Published online: 10 October 2023

Abstract

In structural construction practice, the use of reinforced concrete slabs is extremely common due to their structural and economic advantages. An important issue is the study of structural behavior given to horizontal effects. The significance of this is centered not only on the scales caused by wind and construction loads, which are considered to be "normal" i.e., the quasi-static, which is essentially one-way monotonically increasing but also the most researched seismic, i.e., cyclically varying, direction and magnitude effects. The most widespread methods for sizing flat plate slabs to unidirectional, quasi-static horizontal loads are the so-called Equivalent Frame Method and the Effective Beam Width Method. In addition to analytical and basically linear numerical theoretical methods, several laboratory experiments have been performed and published. In this paper, we investigate the behavior of column-supported flat plate slabs against unidirectional, monotonically increasing horizontal loads using an advanced nonlinear numerical modeling method. Numerical models constructed with different geometric dimensions were created with ATENA 3D three-dimensional nonlinear finite element software. In the numerical studies, in addition to the vertical loads in the global sense, the horizontal loads were also taken into account. In our studies, we analyzed the global behavior of the structure, crack propagation, and internal stresses. The results were illustrated on force - displacement diagrams and compared with the results of the laboratory experiments used, thus showing the accuracy and limitations of the numerical modeling procedure. The numerical results were also compared with the results determined on the basis of the equivalent framework models.

Keywords

non-linear FE, equivalent framework model, effective beam width, reduction factor, column-slab connection, numerical analysis, ATENA software

1 Introduction

Nowadays, in the life of a practicing structural designer, the use of reinforced concrete as a building material is commonplace. Complex material and structural behavior are also sought to be simplified by standards and design practice to make it as applicable as possible in practical design. This approach is negligible, but of course it is fundamentally in favor of safety, so on the one hand it can lead to the construction of less economic structures. On the other hand, in practice the design of flat plate slabs can be said to determine the loads by numerical modeling, but mainly by linearly elastic static calculations. This procedure, as it provides an upper limit on the loads, is acceptable from a design point of view. However, linearly elastic calculations provide a lower bound on the deformations (deflection, rotation, and horizontal displacements), underestimating them, so that the actual structural deformations are not, or only very approximated, even poorly described.

The preliminary calculation of the bracing system of the buildings is basically carried out based on a linear elastic, uncracked theory, for this reason the horizontal displacements of the building only give a lower limit. In our research program, we have developed a procedure in which the non-linear behavior of the structure can be taken into account in fundamentally fast, linearly elastic calculations. Our 3D numerical model is suitable for modeling the non-linear behavior of concrete, the formation of cracks, as well as taking into account reinforcement bars, so the non-linear behavior of the structure can be examined in the results of the 3D finite element calculations. Furthermore, based on the results obtained, it can be

Cite this article as: Roszevák Z., Haris, I. "Finite Element Analyses of Cast-in-situ RC Flat Slab with an Equivalent Frame for Horizontal Loads", Periodica Polytechnica Civil Engineering, 68(1), pp. 289–304, 2024. https://doi.org/10.3311/PPci.21896

taken into account in the linear elastic calculations using the method we have developed.

Among other things, but most of all in terms of the deformations and displacements for the horizontal effects we examined, the widely used linearly elastic modeling methods do not give sufficiently accurate results. In our research, we have developed nonlinear models that more accurately describe real structural behavior, including deformations. We took into account, the characteristics of real rebar, the slip of the reinforcement bar, and the use of nonlinear material models. Research on this topic [1–3] already takes into account the effect of concrete cracking using some reducing factor (β), which has been set based on experimental studies, as it is mostly only for linearly elastic numerical tests and independent horizontal loads separated from vertical loads. The primary purpose of this paper is to find a solution for how it is possible to replace a flat slab supported by columns with a column with an equivalent frame, taking into account nonlinear material properties, based on numerical analysis. In this article, we present the possibilities of numerical modeling of the structural tract extracted and examined from the whole structure.

The numerical modeling method that best approximates the real structural behavior is verified based on the results of an experiment [4], and then a recommendation is made to include the geometric dimensions of the equivalent frame in a preferred case. Our studies basically cover tests with quasi-static vertical and horizontal loads. On some of the models, we also investigated the possibility of modeling horizontal cyclic loads in addition to constant vertical loads based on the results of our previous numerical studies [5]. Based on the results obtained by taking quasi-static horizontal loads, a so-called geometric extension was performed, with which the reduction factor (β) of the replacement frame can be determined in case of different floor plans and geometric designs within the given limits. After extending the method, practicing engineers can perform more accurate scaling in their linear calculations, as the replacement surface can be fabricated and applied with any floor plan layout.

In the following, we present a short literature summary. In engineering practice, the approximate, linearly elastic calculation of flat plate slabs can superimpose the horizontal and vertical loads, taking advantage of this to construct two separate models. Horizontal loads are considered with an equivalent frame (Fig. 1) [6], and vertical loads with column and plate strips on a linearly elastic basis (Fig. 2) [7] and fracture line theory for plastic design. The stresses

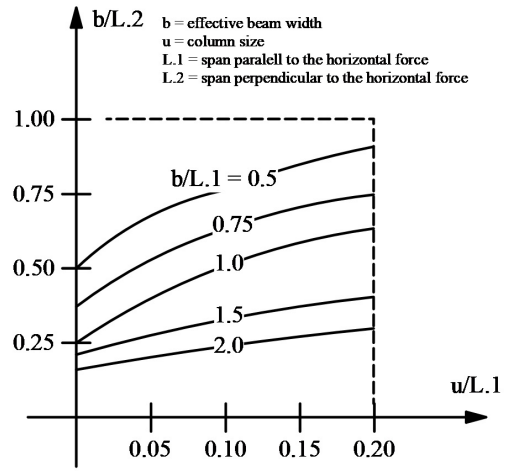

Fig. 1 Effective beam width [6]

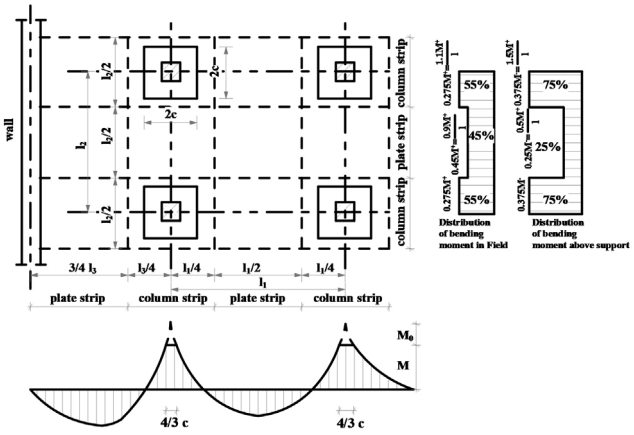

Fig. 2 Definition of the column and plate strip [7]

derived from vertical and horizontal loads, or in the worst case, the separately determined reinforcement quantities, must be summed up on the basis of these, which basically leads to oversizing. From the 1990s onwards, the examination of flat plate slabs with a combination of vertical and horizontal loads was considered.

It was completed in 1993 by Hwang and Moehle [8] an experimental study on the testing of point - supported flat plates for vertical and horizontal loads, which provided the basis for a number of further studies.

In this and subsequent studies, a calculation method for designing flat plates that best approximates reality, but it is basically linear, and it was sought already in terms of describing deformations.

These methods include the Effective Beam Width Method (Fig. 3) and the Equivalent Frame Method (Fig. 4). Both methods describe the reduction in stiffness during the actual behavior of the structure, the appearance and effect of cracks, using an individually defined reduction factor (β).

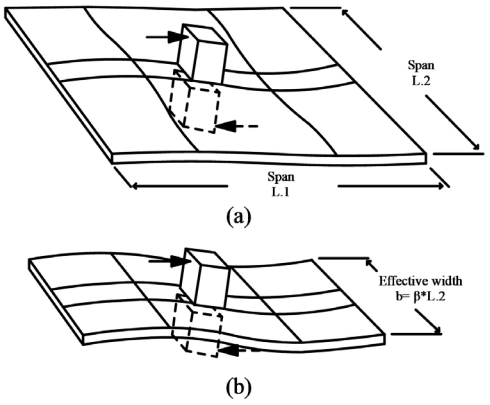

Fig. 3 Effective beam width [2] (a) column-slab connection, (b) effective beam width

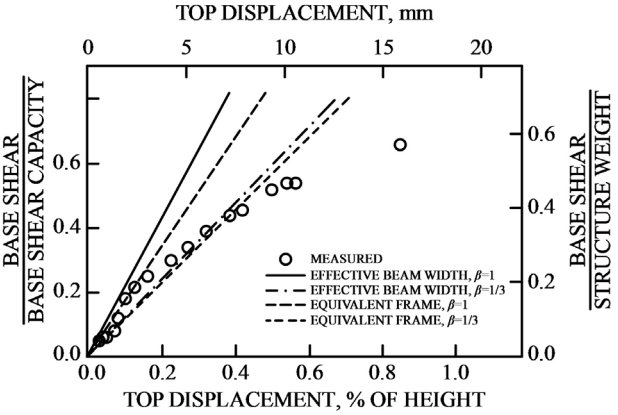

Fig. 4 Results of the EBWM and EFM

The methods continue to use linearly elastic computation. Full beam width is taken into account in stress state I (non-cracked) (Fig. 4). In the larger and plastic deformation ranges, stress state II., a reduced stiffness is already offered, which also means a replacement, reduced beam width to be considered in linearly elastic calculations.

Several studies [4, 9, 10–13] deal with the accuracy of these two methods and the analysis of their usability limits. These studies agree that the two methods involve significant neglect and can only be applied to the stiffness range in the elastic range with a horizontal load. Furthermore, the effective elastic stiffness is provided by the upper estimate of the Effective Beam Width Method and the lower estimate of the Equivalent Frame Method. Overall, these methods are inaccurate and have limited applicability in design practice.

The development of finite element technology, but most of all software, in numerical studies of the subject has not brought about a proportional development. There have been few numerical, nonlinear, finite element studies in the literature to date [1, 9]. The few modeling procedures have not been compared and verified with the many experimental results available, even for a one-way monotonically increasing quasi-static load.

At the same time nowadays, several laboratory studies are concerned with the examination of flat plate slabs for cyclically varying loads of varying direction and magnitude. Zhou and Hueste [14] performed experimental studies on vertical and cyclically varying horizontal loads to understand the behavior of an intermediate column-to-plate connection.

2 Numerical study

2.1 Quasi-static analyses

In the following, we present two numerical modeling methods for reinforced concrete slabs. The first modeling procedure was developed in the three-dimensional nonlinear finite element program ATENA 3D. This family of programs is specifically designed for nonlinear testing of concrete and reinforced concrete structures but is not yet widespread in the wider engineering community. The models and modeling method developed for the unidirectional monotonically increasing test case loaded with quasi-static load were verified using a laboratory experiment [4]. Quasi-static analyses were performed using the modeling procedure we developed [15–20].

In addition to the ATENA software package, we also used AxisVM, the most widespread finite element software in some European countries, to calculate the recommended equivalent frames, which was used to perform the proposed linear static calculations.

The investigated structure consists of the excavated part of the general intermediate level of a building made of columns and flat slabs (Fig. 5). The basic data of the numerical analyses are summarized in Tables 1 and 2.

The model built in the ATENA software has a doubly symmetrical floor plan, so a general two-way, so-called contains plate and column bars. In the numerical models, there are two columns, modeled between the half-level elevations below and above the examined slab, the inflection points per level. The half-columns have a cross-sectional dimension of $u \times u$, a length of 1.5 m and a distance of L.1–L.2 (Fig. 5). The thickness of the reinforced concrete slab is v and the reinforcement used is shown in Fig. 5.The geometry of the models are shown in Table 3. The applied reinforcement was determined using finite element software, taking into account the loads reported later.

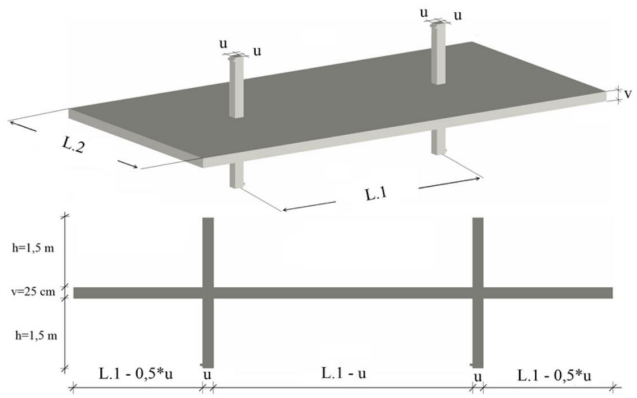

(a)

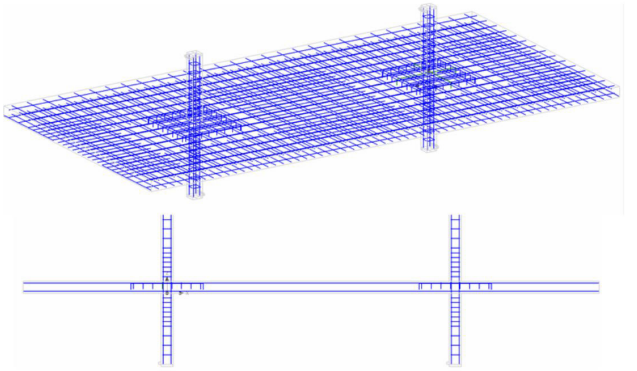

(b)

Fig. 5 ATENA model, geometry, (b) reinforcement

Table 1 Basic data of the specimens - column

Longitudinal reinforcement in the column	Stirrups in the column
2 × 4 Ø20	2 × 20 Ø8/100/200

Table 2 Basic data of the specimens - slab

Reinforcement in the slab (up and bottom)	Additional reinforcement in the slab (bottom)	Additional reinforcement in the slab (up)
Ø12/300/300	Ø12/300/300	2x16Ø16/150/150

During our numerical studies, we also developed two types of nonlinear modeling methods based on the different modeling of the reinforcement bars [5]. In the first case, we used a linearly elastic and linearly hardening idealized material model, while in the second case, we used a material model characteristic following the real reinforcing steel behavior.

This was necessary because the hardware requirements and computational time of the procedure containing real material models are significantly longer than in the idealized case. In our "real nonlinear" numerical model, we also considered the effect of slip on rebar steels [5]. The "C25/30 mean values" material model was parametrized for the concrete structural elements, which is a nonlinear material model that can be used in the ATENA program package.

Table 3 Geometry of the models

Model number	Thickness of the slab v [cm]	Size of the column u [cm]	Span direction X L.1 [m]	Span direction Y L.2 [m]
1	25	25	6	6
2	25	25	7	5
3	25	25	5	7
4	25	25	8	4
5	25	25	4	8
6	25	20	6	6
7	25	20	7	5
8	25	20	5	7
9	25	20	8	4
10	25	20	4	8
11	25	30	6	6
12	52	30	7	5
13	25	30	5	7
14	25	30	8	4
15	25	30	4	8
16	20	25	6	6
17	20	25	7	5
18	20	25	5	7
19	20	25	8	4
20	20	25	4	8
21	20	20	6	6
22	20	20	7	5
23	20	20	5	7
24	20	20	8	4
25	20	20	4	8
26	20	30	6	6
27	20	30	7	5
28	20	30	5	7
29	20	30	8	4
30	20	30	4	8
31	30	25	6	6
32	30	25	7	5
33	30	25	5	7
34	30	25	8	4
35	30	25	4	8
36	30	20	6	6
37	30	20	7	5
38	30	20	5	7
39	30	20	8	4
40	30	20	4	8
41	30	30	6	6
42	30	30	7	5
43	30	30	5	7
44	30	30	8	4
45	30	30	4	8

To establish the relationship between the loading horizontal force and the reinforced concrete column, an intermediate steel contact element was defined, which was described using an isotropic, linearly elastic material model. The geometric design of the model is given in such a way that it follows the behavior of the real structure. This was achieved by means of columns and supports defined at the edges of the plates (Fig. 6).

Vertical loads were defined as distributed forces on the structure. Distributed loads (W) with an intensity of 6.25 kN/m^2 corresponding to the self-weight loads and (F_v) 720–720 kN for the columns, but smeared on the pillar cross-section, were modeled on the plate. The latter corresponds to ~ 70% of the column load-bearing capacity.

During the numerical analyses of the models, the vertical loads were applied to the model in the first 5 load steps, after which the horizontal loads were operated through contact elements placed at the bottom of the columns in 5–5 kN (F_h) horizontal load (in the direction X) increments. The vertical load is operated with a constant value after the 5th load step during the horizontal load.

The number of load steps has been determined so that the horizontal displacement on the structure exceeds the 10 mm value we expect. During our investigations, we detected displacements due to the force applied to the bottom of the columns.

Tests with nonlinear numerical models in the ATENA software package are required to determine the equivalent beam width of the replacement frame. With this in mind, we have the opportunity to obtain results that are linear and elastic in terms of deformation, which are closer to real structural behavior.

Using AxisVM, we created a frame model with alternate geometric dimensions that we determined to describe the horizontal displacements in a linearly elastic manner, but we determined to describe the horizontal displacements based on the nonlinear numerical results. In the model, both the columns and the equivalent plate field were given as beam elements. The aim was to use surrogate equivalent cross-sectional dimensions that could be determined from more advanced nonlinear, numerical results on a software that is more common among practicing engineers.

The supports were also designed based on the boundary conditions required for symmetry, so vertical and horizontal supports were set on the columns (Fig. 7).

The vertical loads are given as dead weights and the forces V are indicated in Fig. 7. The value of the vertical forces is the same as the forces (V) of 720–720 kN defined

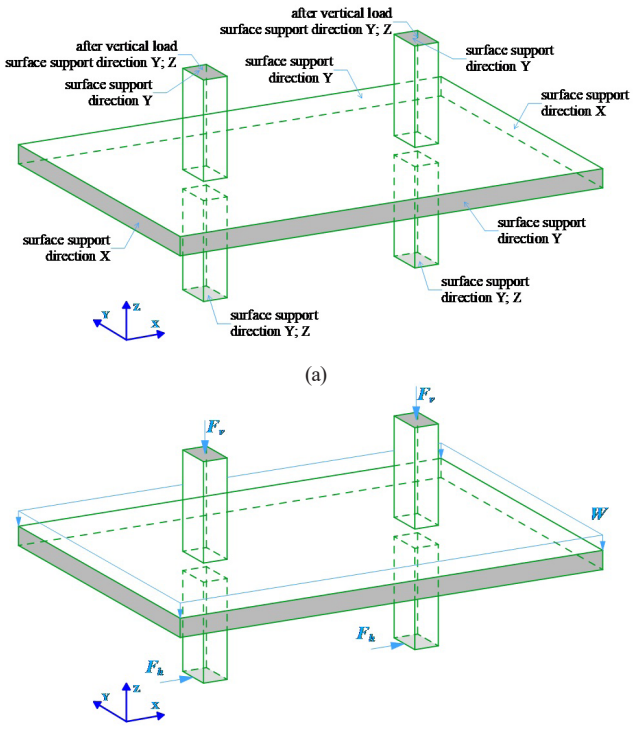

Fig. 6 Loads and support of the models (a) supports, (b) vertical and horizontal loads

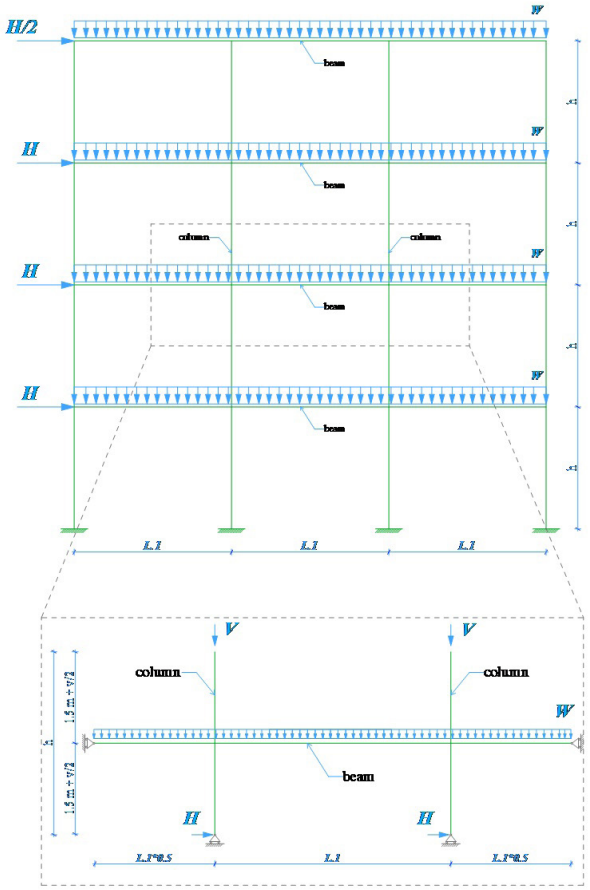

Fig. 7 Interpretation of static structure and loads

in the ATENA program. The load distributed on the surface loading of the slab was divided into the beam as a load distributed along the line (*W*) see in Fig 7. The horizontal forces (*H*) are given in the plane of the frame, and it was placed at the bottom of the columns (Fig. 7). The resulting horizontal displacements were determined on the replacement beam model.

2.2 Cyclic analyses

Cyclic studies were performed using the modeling procedure we developed [5]. The material for concrete shown in Fig. 8 was used. For tensile (fracture) and compressive (plastic) behavior, the software applied a smeared crack approach in respect of the concrete junction using a fracture plastic model.

The fracture model is based on the classical orthotropic smeared crack band and crack formulation model [21, 22]. Rotating and fixed crack models can be used in relation to exponential softening and Rankine tensile failure criterion. The plasticity for concrete in compression is inspected by the Menetery-Williams failure surface [23]. The failure surface in compression is expressed in terms of three (independent) stress invariants such as hydrostatic stress, deviatoric stress, and deviatoric polar angle. The compressive strength of the concrete (f_c = 27.58 MPa, f_t = 2.19 MPa, G_f = 5.47*10^{-5} MN/m) is defined in the same way as in the quasi-static analyses. The reinforcement is defined by the cyclic properties based on the Menegotto-Pinto model (Menegotto and Pinto [24]) (Fig. 8). The yield strength (f_y = 413.6 MPa) and tensile strength of the reinforcement bars are also the same as in the quasi-static tests. In the longitudinal bars placed in the beam, the effect of slipping is taken into account. However, the perfect connection for the stirrups and the bars is set in the beam. In cases where the slip of the reinforcement bars is taken into account, the relationship between the concrete and the reinforcement bars is defined by a memory bond parametrized model (τ_f = 5.25 MPa). For the bond-slip relationship (Fig. 8), the model is taken according to the CEB-FIP Model Code 1990 [25]. The placing of the bars is defined in the same way as in quasi-static tests.

Different parameterization is required for modeling cyclic behavior, thus ATENA adds a so-called Unloading Factor to model concrete behavior under cyclic loading. The Unloading Factor controls crack closure stiffness. The factor mainly influences the shape of the hysteresis curve; in our analyses, the parameter was set to zero because this value provides the best fit to real behavior [5].

Fig. 9 shows the direction of the positive and negative load as well as the horizontal force (F_h) and the measured displacement (*e*). In the quasi-static test, the constant vertical force (F_v) at the top of the column and the vertical load (*W*) on the slab were also defined, and it was the same as in the quasi-static analyses (Fig. 9). Cyclic tests were performed on the Model 1. only. A novelty in the parameterization of the models is that we have reduced the fixed crack coefficient (c_{fr}) from 1.00 to 0.8. To study the cyclic behavior, 4 models were developed, which we defined with different displacement limits. The structure and the parametrization of the models are exactly the same, the

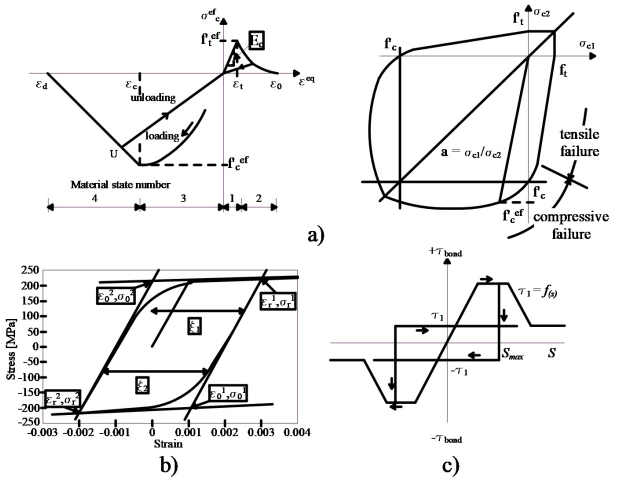

Fig. 8 Material properties (a) concrete material model, (b) cyclic reinforcement model, (c) bond-slip relationship [23]

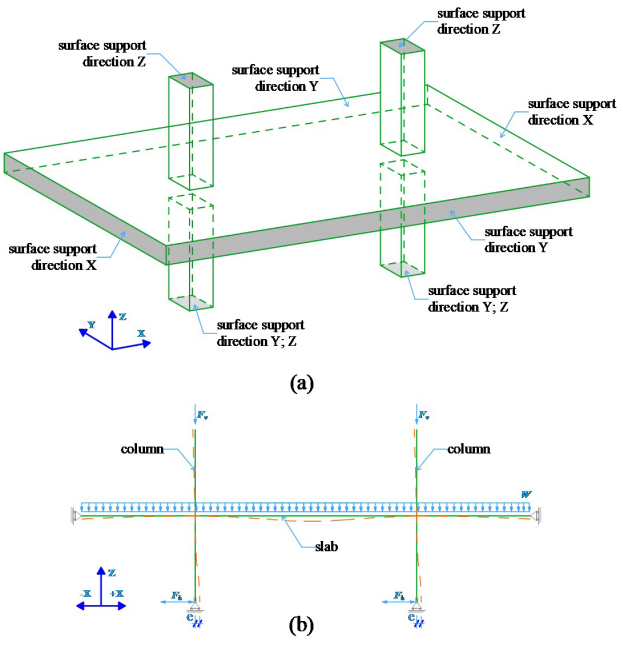

Fig. 9 Static structure and supports (a) support conditions, (b) direction of the loads

only difference is the degree of load. The applied limits are adjusted to the values of the displacements determined in the quasi-static tests, so we defined (horizontal) displacement loads of 1, 4, 7, and 10 mm.

2.3 Numerical properties

Based on our previous study [7], the finite element division was designed so that the cross-section of a column had a minimum of four and the cross-section of the slab two finite elements should be avoided. In the numerical model, quadratic (slab) and linear (columns, coupling elements, reinforcement) base functions were used alternately between the structural elements.

For the concrete elements the 20-node solid (CCIsoBrick) finite elements were used for the reinforcement 2D truss (CCIsoTruss) elements were used [23] (Fig. 10.). For all nonlinear analyses, an iterative method (Newton-Raphson iteration method) was used to perform the iteration process. The Cholesky resolution was used to solve the state equation of the structure.

3 Numerical analyses and results

Linearly elastic static calculations give the lower limit of stresses and the upper limit of deformations in the case of cracked reinforced concrete structures. The results are presented based on the results of Model 1, which can be used to determine the equivalent frame model for a given geometry. It can be seen in Fig. 10 that the linear and nonlinear models give nearly identical results in the initial cracked state, however, leaving the linear elastic limit changes. In addition to the standard load-bearing structures, monolithic reinforced concrete structures crack in the serviceability limit state. The purely linearly elastic calculation, with its initial geometrical dimensions, may not be suitable for describing the actual deformations of the structure, in this case the horizontal displacements. Therefore, there is a need to develop nonlinear numerical models and, after verifying them, return the results to linearly elastic modeling.

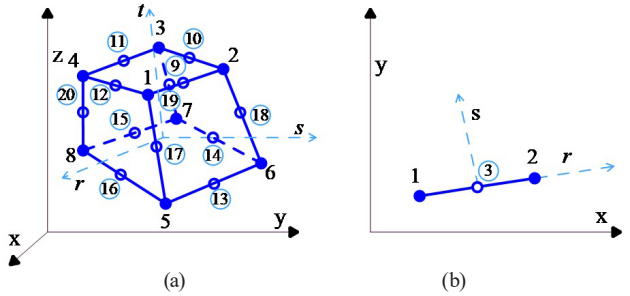

Fig. 10 Finite elements (a) CCIsoBrick, (b) CCIsoTruss [23]

In the following, we give the results obtained during our linearly elastic (AxisVM) and two nonlinear (ATENA 3D) numerical studies developed by us. In the latter case, the results of the models constructed with the idealized ("idealized nonlinear") and the real rebar characteristic ("real nonlinear") are described separately. The resulting force-displacement diagrams are shown in Fig. 11.

As expected, the numerical results in stress state I are almost the same. After cracking, the results of the linearly elastic and nonlinear models differ significantly, also as expected. In nonlinear models, there will be a decrease in stiffness describing the nature of the actual behavior, resulting in larger horizontal displacements. The Fig. 11 clearly shows the limitation of the applicability of linearly elastic calculations for displacement.

The nonlinear behavior of the 3D nonlinear model can be observed not only in the force-displacement diagram, but also in the stress and deformation diagram presented in Fig. 12. In the Fig. 12., the cracks formed due to the horizontal load are also shown, which clearly proves that the appearance of cracks is also taken into account in the 3D nonlinear model.

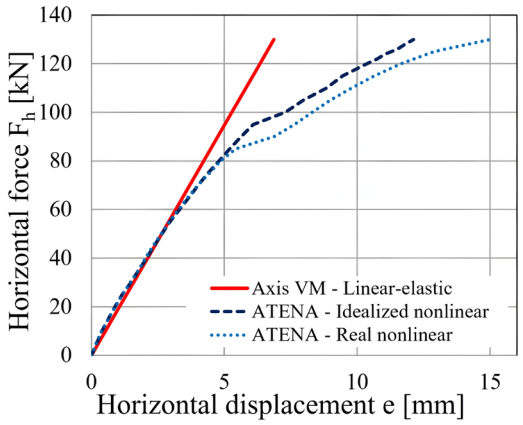

Fig. 11 Force-displacement diagrams, taking into account the full slab width

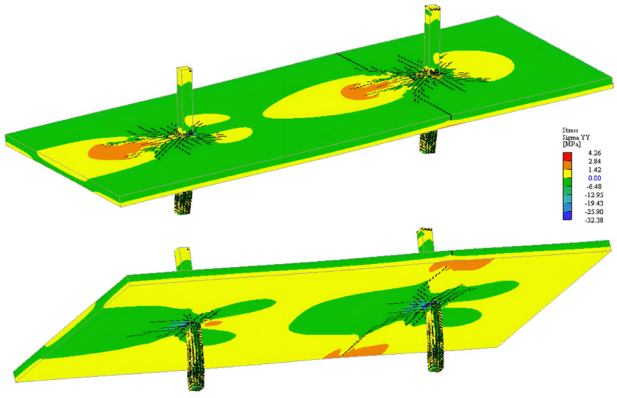

Fig. 12 Stress figure (Sigma YY) and crack pattern

From the obtained results, it can be clearly stated that only the nonlinear modeling methods alone can describe the nature of the real behavior after cracking [20].

To select a nonlinear modeling method that more accurately describes the actual behavior, it becomes necessary to compare the results obtained with real-world laboratory experiments, which are described in the next section.

3.1 Comparison of laboratory and numerical experimental results

Our developed numerical method [5, 16] is verified based on a real laboratory experiment [4]. We have already built our numerical models according to the test specimens used in the laboratory experiment used [4]. We remark that in the publication, the enclosing geometric and material characteristics were available to us, but the actual amounts of reinforcement were not.

The ratio of the horizontal and vertical forces of the bidirectionally symmetrical, general intermediate slab section is compared (Fig. 12). The comparison is performed using the diagram published by the authors of the laboratory experiment [4]. As shown in Fig. 13, the results of the laboratory experiment and the analysis obtained with numerical models follow each other well.

It can be seen in Fig. 13 that in the initial cracked state, all three models have similar stiffness, and then the experimental model suffers a greater stiffness reduction than the numerical models. As a result, there is a ~ 10% deviation in horizontal forces with the same offset (~ 5mm) [16]. At this stage, the two numerical models behave similarly. In the displacement range beyond this, the "real nonlinear" numerical model suffers a greater stiffness reduction than the "idealized nonlinear" model, as a result of which the laboratory experiment and the "real nonlinear" numerical models follow each other well at shifts above ~6 mm. They suffer the same displacement under horizontal force. In this range, the difference of the "ideal nonlinear" model from the laboratory experiment is ~9–10%, while the difference of the "real nonlinear" model is ~2–3% [20].

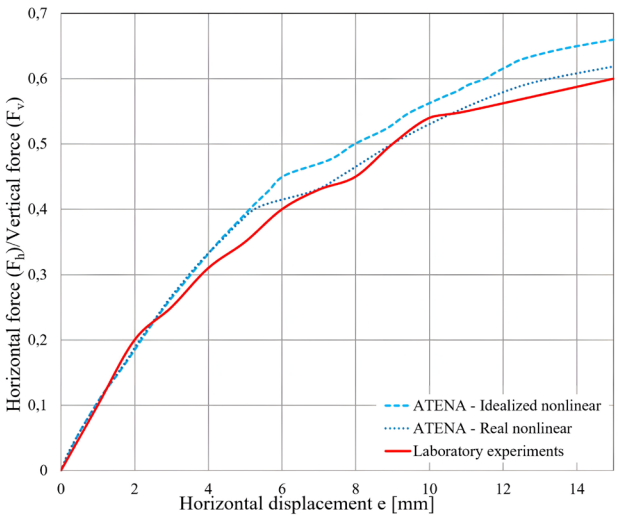

Fig. 13 Comparison of the laboratory experiments and the numerical results

Based on these, it can be concluded that using our "real nonlinear" numerical model gives a better result compared to the laboratory experiment than our "idealized nonlinear" model. However, the downside to this setup is that it requires more computing power, which is twice the runtime.

3.2 Replacement equivalent framework model

The replacement equivalent frame model is a linearly elastic approximation method for calculating point-supported reinforced concrete slabs. The model is based on nonlinear analysis in the ATENA software. The force-displacement pairs thus obtained must be reproduced by varying the parameters of the linearly elastic model. For the replacement equivalent frame model, this parameter is the size of the equivalent beam width.

The steps for determining the equivalent beam width, based on the verified nonlinear modeling procedure, are described below. Our primary criterion is to adjust the replacement width of the linear model, which cannot follow the stiffness reduction so that the whole frame is the same as the displacement result of the nonlinear model in the predetermined behavioral stages. The equivalent beam width was determined by an iteration procedure using AxisVM software. As the loads increase, we reduce the replacement beam width of our frame model so that the stiffness of the linear numerical model against the horizontal load is numerically equivalent to the result of the nonlinear model that accurately approximates the real behavior. Only the equivalent beam width was changed/reduced, all other parameters, according to the initial conditions, remained unchanged. Finally, the so-called reduction factor (β_i) was determined.

This is completely analogous to the results of analytical solutions found in the literature [4, 9].

By implication, the previous method can be generated numerically at each force-displacement point, so that it can even be described as a function in a continuous form. Performing on the models we have defined, these force-displacement point pairs can be generated on a two-dimensional surface, shown below. Based on the detected horizontal

displacements, we approximated the total force-displacement diagram with approximately five highlighted points (I, II, III, IV, and V) and five linear sections. The value of the reduction factor (β_i) can be given as the quotient of the specified equivalent plate width and the column spacing perpendicular to the force (600 cm). The equivalent beam width was determined to the nearest 5 cm in the AxisVM software. The results obtained and the reduction factors are summarized in Table 4.

In the first section, it can be seen that the equivalent slab width is equal to the distance perpendicular to the force of the columns ($\beta_I = 1$), which corresponds to the original, non-cracked state. The second range (1–4 mm), which shows relatively small displacements, can be described as a slight stiffness reduction with a reduction factor of $\beta_{II} = 0.67$. II. and III. (4–7 mm), the dominant plastic deformations appear in the third stage. The equivalent plate width that can be considered is already drastically reduced ($\beta_{III} = 0.38$). An III. and IV. (7–10 mm), in the third stage, our model is already characterized by significant plastic deformation.

In the fourth stage, the equivalent plate width that can be considered decreases even more ($\beta_{IV} = 0.23$). The range IV. corresponds to the average allowable relative level shift value, which in our case is H / 300 = 10 mm.

At the V. point, the reduction factor (β_V) is only 0.13 compared to the initial value of 1.0. The experiment was carried out up to the value of the relative inter-story drift (inter-story drift = 1%) allowed according to EN 1998-1, so the largest shift was 15 mm (H/2 * 1% = 15 mm).

The displacement at the end of the section already not means the displacement due to failure.

The force-displacement diagram of our "real nonlinear" numerical model is shown in Fig. 14, with the five highlighted points.

In Fig. 15, the force-displacement diagram of the "real nonlinear" model is approximated at 5 selected points, giving the reduction factors (β_i) to be applied to these points during the given displacement. Of course, the reduction factor of the force shift during intermediate displacements could also be determined for point pairs, but this will be presented in a later section. Fig. 16 respectively illustrates the difference between the approximated curve and the "real nonlinear" model force-displacement diagram. Based on these, it can be seen that the average difference between the two curves is only ~1–2% [16].

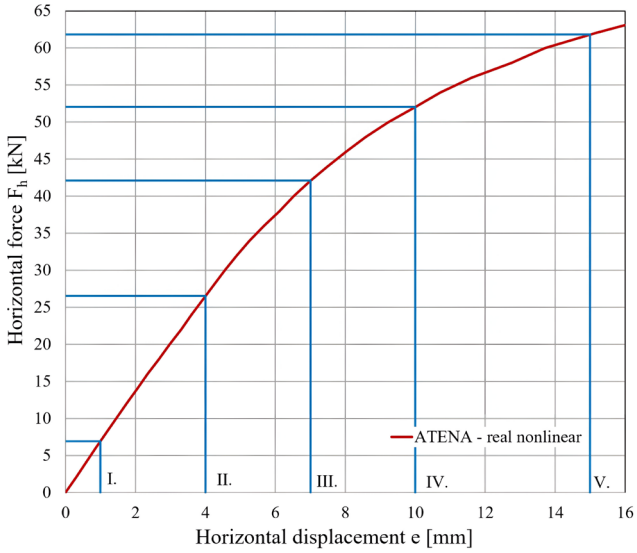

Fig. 14 Load-displacement diagram for real nonlinear model

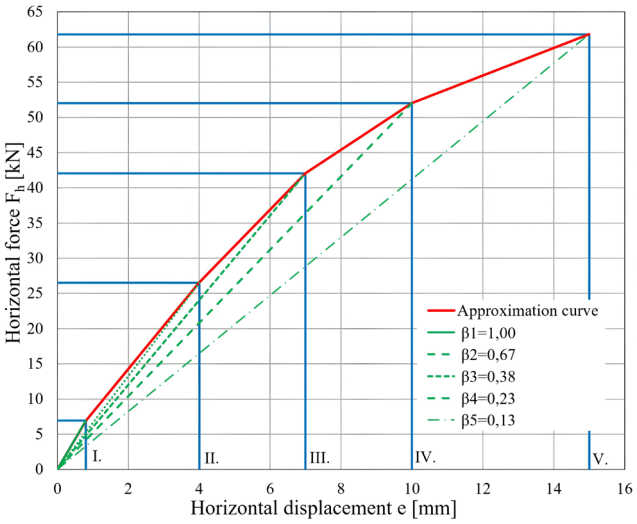

Fig. 15 Five sections approximated load-displacement curve

Table 4 Geometry of the models

Highlighted point	Horizontal displacement e_i [mm]	Ratio of the relative total displacement [%]	Horizontal load F_i [kN]	Ratio of the relative load [%]	Replacement beam width B_i [cm]	Reduction factor β_i [-]
I.	1.0	7	6.93	11	600	1.00
II.	4.0	27	26.53	43	400	0.67
III.	7.0	47	42.08	68	230	0.38
IV.	10.0	67	52.03	84	135	0.23
V.	15.0	100	61.82	100	80	0.13

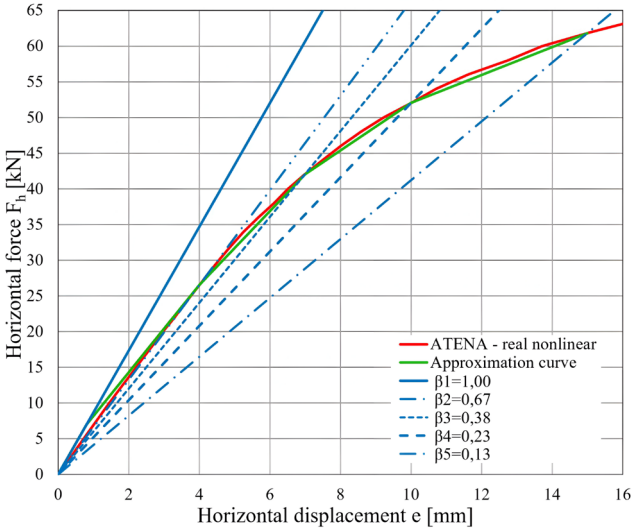

Fig. 16 Numerically produced load-displacement diagrams

The results presented so far serve as a representative sample with a distinguished geometric design, which shows that the flat plate slab supported at the points can be examined with the method we use and the (β_i) reduction factor can be given. Not only with the geometry we use, but also with different floor plan proportions, so in the end, a 3D surface can be produced for a given structure. With this method, complicated nonlinear modeling can be avoided, but more accurate results can be obtained than with general linear modeling, especially with respect to deformations.

3.3 Geometric extension of a replacement equivalent frame model

With the numerical models we examined, the models created with the selected geometry can be analyzed. Using the numerical modeling procedure we developed, we performed the numerical models, which were grouped by the ratio of the grids. Our goal is to be able to determine the reduction factor for any structural geometry by the geometries we study. To do this, we summarize the results obtained with the defined models. Based on the aggregated results, the values of each variable and the reduction factor can be plotted on a 3D graph to which a 2D interface can be fitted.

The replacement beam width can thus be extended to any geometry according to the specified grid ratios. As a first step in the extension, the results obtained with each variable parameter (slab thickness: v, column size: u, raster ratio: L2/L1) are plotted on force-displacement graphs, see Fig. 17.

Evaluating the results, we determined the differences from the initial Model 1., summarized in Table 5. In the table, we give the results for each of the preferred displacements and their deviations.

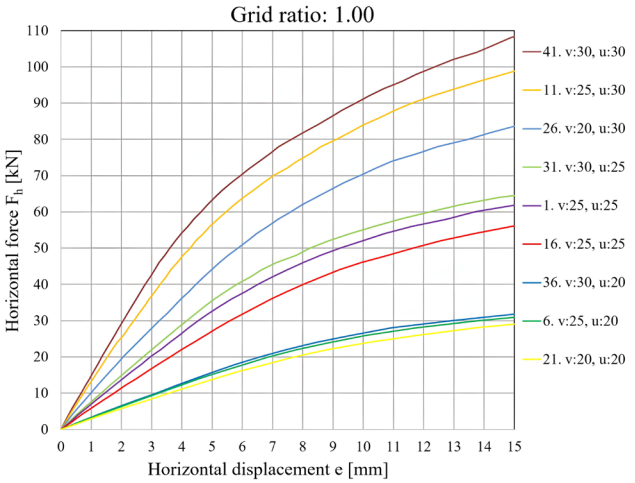

Fig. 17 Summary of numerical results – grid ratio: 1.00

The tests were evaluated in each case against Model 1. Compared to model 1., where the slab thickness is 25 cm and the column size is also 25 cm, the models with the largest slab thickness (v = 30 cm) and column (u = 30 cm) cross-section show a difference of up to -75 and -115%. The models with the smallest slab thickness (v = 20 cm) and column (u = 20 cm) cross-section defined by us show a difference of between 53 and 58% in terms of the preferred displacements.

Based on our studies, we determined 5 grid ratios, two extreme values, and 3 internal ratios between them, see Table 6. For each grid ratio, the results presented above were performed and the results of models with the grid ratios, but different parameters were plotted on a 3D graph. For the sake of representability, the axles included the v/u (slab thickness/column size) ratio, the displacement, and the reduction factor.

In the following, we present 3D graphs of the ratio of grid distances, on which the (β) reduction factor can be determined as a function of each v/u ratio and a specific displacement value. Based on our studies, we performed two-variable interpolation for the results obtained at discrete points, which was used to determine a two-dimensional continuous surface. Polynomial regression was used to construct the two-dimensional surfaces, see Figs. 18, 19, 20, and 21 for the results obtained.

Based on the fits, we generated their functions, which are described below:

$$\beta\left(\frac{v}{u},e\right)=0.425-0.2924\left(\frac{v}{u}\right)-0.07382e+0.1014\left(\frac{v}{u}\right)^2 -0.0483\frac{v}{u}e+0.008297e^2, \quad (1)$$

if L2/L1 = 0.5.

Table 5 Comparison of force-displacement curves

Model umber	Horizontal force F [mm]	Difference [%]	Preferred displacement
41.	14.77	-113	
11.	13.16	-90	
26.	10.10	-46	
31.	7.61	-10	
1.	6.93	0	1 mm
16.	5.83	16	
36.	3.34	52	
6.	3.23	53	
21.	2.92	58	
41.	54.16	-104	
11.	47.59	-79	
26.	36.17	-36	
31.	28.86	-9	
1.	26.53	0	4 mm
16.	22.06	17	
36.	12.65	52	
6.	12.22	53	
21.	11.11	58	
41.	76.60	-82	
11.	69.82	-66	
26.	58.00	-38	
31.	45.48	-8	
1.	42.08	0	7 mm
16.	36.09	14	
36.	21.04	50	
6.	20.24	52	
21.	18.43	56	
41.	91.12	-75	
11.	83.94	-61	
26.	70.41	-35	
31.	55.08	-6	
1.	52.03	0	10 mm
16.	46.14	11	
36.	26.56	49	
6.	25.80	50	
21.	23.75	54	
41.	108.29	-75	
11.	98.81	-60	
26.	83.57	-35	
31.	64.49	-4	
1.	61.82	0	15 mm
16.	56.11	9	
36.	31.78	49	
6.	30.91	50	
21.	29.00	53	

Table 6 Summary table of test ranges

Grid ratios L2/L1	Grid L1	Grid L2
0.5	8.00	4.00
0.71	7.00	5.00
1.00	6.00	6.00
1.40	5.00	7.00
2.00	4.00	8.00

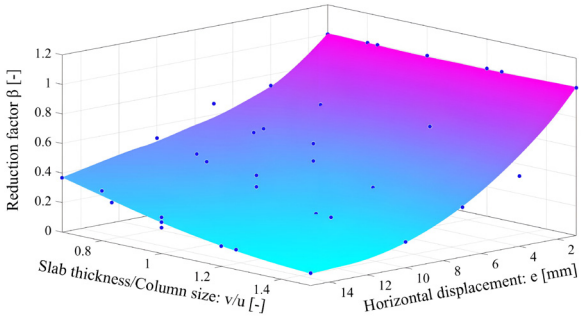

Fig. 18 Graph of the reduction factor (β) – grid ratio: 0.50

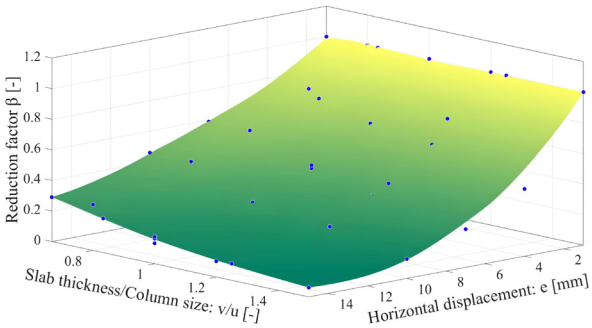

Fig. 19 Graph of the reduction factor (β) – grid ratio: 0.71

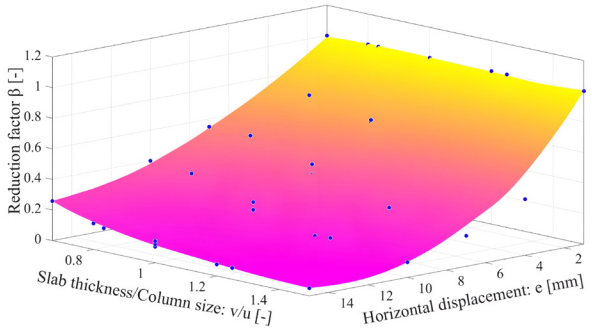

Fig. 20 Graph of the reduction factor (β) – grid ratio: 1.00

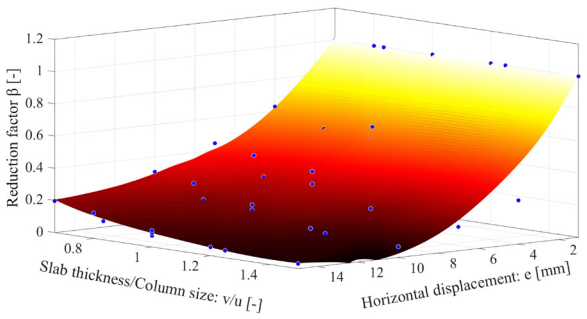

Fig. 21 Graph of the reduction factor (β) – grid ratio: 1.40

$$\beta\left(\frac{v}{u},e\right)=0.4065-0.3157\left(\frac{v}{u}\right)-0.0702e+0.1(\frac{v}{u})^2 \\ -0.04431\frac{v}{u}e+0.00644e^2, \quad (2)$$

if L2/L1 = 0.71.

$$\beta\left(\frac{v}{u},e\right)=0.3417-0.337\left(\frac{v}{u}\right)-0.08016e+0.1201(\frac{v}{u})^2 \\ -0.04406\frac{v}{u}e+0.007002e^2, \quad (3)$$

if L2/L1 = 1.00.

$$\beta\left(\frac{v}{u},e\right)=0.244-0.3518\left(\frac{v}{u}\right)-0.05787e+0.1643(\frac{v}{u})^2 \\ -0.0389\frac{v}{u}e+0.008654e^2, \quad (4)$$

if L2/L1 = 1.40.

3.4 Results of the cyclic analyses

The cyclic tests were performed with 4 displacement limits of different magnitudes, for which see load history diagrams in Fig. 22. The maximum displacement limit was taken on the basis of the limit set for the reduction of deformations, which is also in line with those given in the international standards [26–29]. Based on the geometric structure of the models, we maximized the maximum displacement limit by 10 mm. In order to determine the (β_{cyc}) reduction factor, the models were constructed with the displacement values used for the quasi-static tests, so that the difference between the quasi-static and the cyclic analyses could be determined.

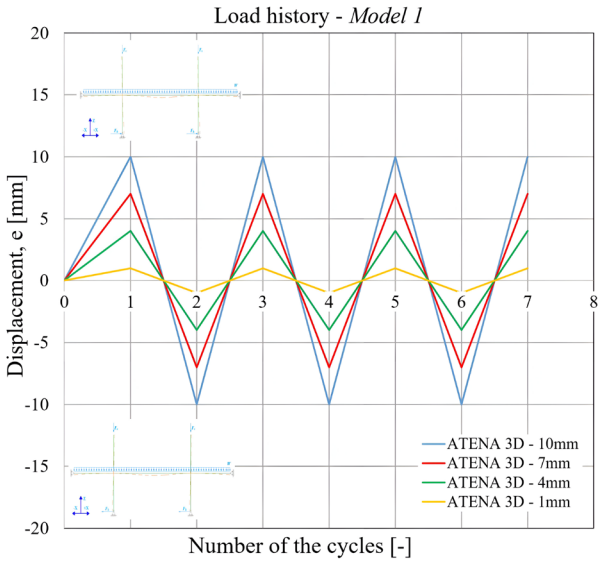

Fig. 22 Load history for cyclic analyses

We illustrate the results obtained with the modeling technique we developed on a force-displacement diagram, see Fig. 23. Hysteresis loops characteristic of cyclic behavior can be observed in the obtained force-displacement diagrams. Furthermore, cyclic degradation can be modeled with the developed modeling technique. At low displacement values (1 and 4 mm), the value of the peak force generated at the end of the loops does not show a significant decrease. However, in the case of larger displacements in terms of structure (7 and 10 mm), a significant reduction in peak force can be observed from an engineering point of view. The force values detected at the end of each cycle are summarized in Table 7.

Based on the available results, we determined the (β_{cyc}) reduction factor for each displacement limit, taking into account the cyclic behavior. In the case of positive and negative loads, the reduction factor can be determined, whichever the smaller one should be used. Based on the numerical tests, it can be concluded that the finite element model is sensitive to the direction of the load because higher force values can be achieved in the starting direction at

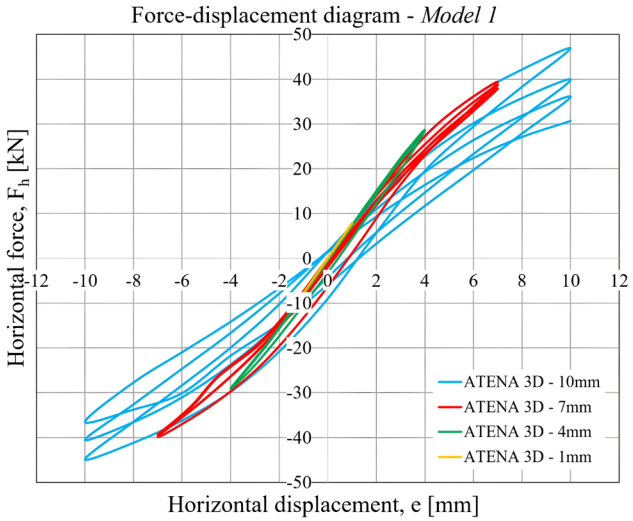

Fig. 23 Force-displacement diagram – results of the cyclic analyses

Table 7 Summary table of the results

Number of cycles	Horizontal force F_h [mm]			
	1 mm	4 mm	7 mm	10 mm
1.	7.85	28.64	39.38	46.85
2.	-7.85	-29.14	-39.87	-44.86
3.	7.85	28.53	38.70	39.85
4.	-7.85	-29.02	-39,67	-40.51
5.	7.85	28.43	37.88	36.06
6.	-7.85	-29.02	-39.37	-36.50
7.	7.85	28.43	37.85	-30.65

the same displacement levels. To determine the reduction factor, we selected the force levels illustrated in Fig. 24. In the positive and negative directions, the reduction factors for each displacement level were determined based on the force-displacement point pair measured in the two subsequent cycles.

Based on the results, we determined a coefficient (r_{cyc}) for modifying the reduction factor to take cyclic behavior into account. In Table 8., we summarized the values of the forces obtained in the first and last cycles and gave their deviations. In the positive and negative directions, the value of the modification factor is different, which is illustrated in Fig. 25.

In terms of results, we propose to include the smaller value of the modification coefficient (r_{cyc}) for the calculation of the reduction factor (β) by approaching the safety advantage. Thus, the following formula can be used to calculate the reduction factor (β_{cyc}) given to take account of cyclical behavior:

$$\beta_{cyc} = r_{cyc} \times \beta \,, \tag{5}$$

where:

β_{cyc} reduction factor for cyclic analyses,
β reduction factor for the equivalent beam width,
r_{cyc} coefficient for modifying the reduction factor.

The modification coefficient (r_{cyc}) was determined on the basis of only one model (Model 1.), however, the modeling technique developed by us can be used to perform cyclic studies in the case of other models examined during the research, from which the modification coefficient (r_{cyc}) can be determined for models with different geometries.

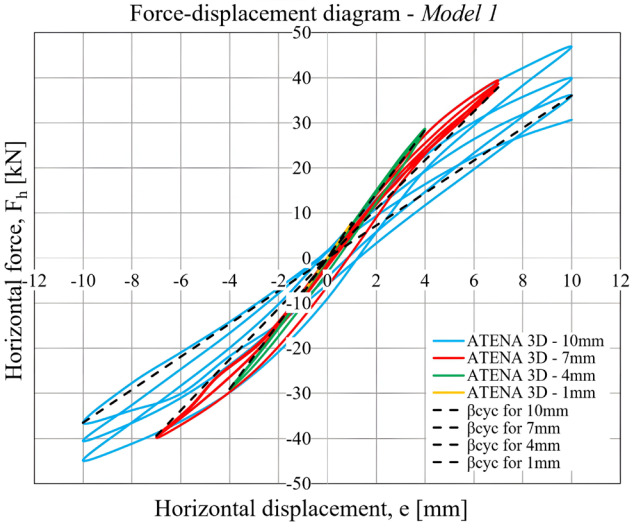

Fig. 24 Force-displacement diagram – reduction factors

Table 8 Summary table of the results

Number of cycles	Direction of the load	Horizontal force F_h [mm]			
		1 mm	4 mm	7 mm	10 mm
1.	positive	7.85	28.64	39.38	46.85
7.	positive	7.85	28.43	37.85	-30.65
Modifying coefficient r_{cyc}		**0.000**	**0.993**	**0.961**	**0.654**
2.	negative	-7.85	-29.14	-39.87	-44.86
6.	negative	-7.85	-29.02	-39.37	-36.50
Modifying coefficient r_{cyc}		**0.000**	**0.996**	**0.987**	**0.814**

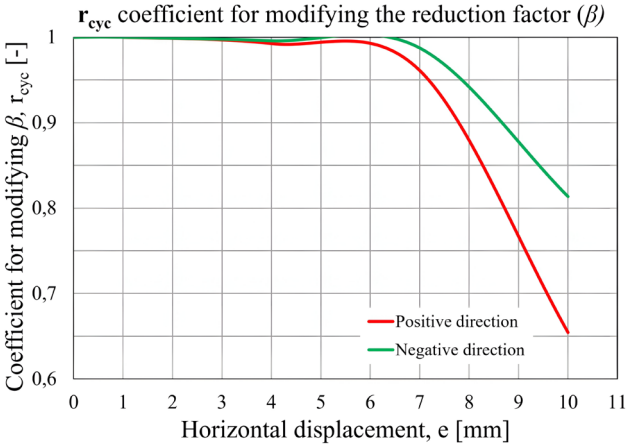

Fig. 25 r_{cyc} coefficient for modifying the reduction factor β

4 Conclusions

We have shown that the numerical modeling method we have developed is suitable for the analysis of point-supported flat plate slabs under vertical and horizontal loads. The horizontal force displacement results obtained with the described modeling procedure were compared with a laboratory experiment found in the literature [4]. We have shown that the deviation of the method from laboratory experiments is 5–10% in the case where the real material characteristics are modeled. Using the verified numerical model, we showed in a geometric arrangement identical to the laboratory experiments that a linear computational framework model approximating the results of nonlinear numerical experiments describing the behavior of flat slabs supported by columns can be generated using an equivalent beam width. The modeling technique we have developed can be used to more accurately model the real behavior of the structure, especially with respect to significant plastic deformations. The methods found in the literature are mostly linear test methods, which give significant inaccuracies after the cracking of the concrete, especially in the field of deformations. In our studies, the geometry and load levels, especially the vertical load, were determined so that the constructed models were not sensitive to punching shear.

The phenomenon of punching shear was not addressed in the studies performed. In addition to the material characteristics, we have parameterized in the models and the reinforcement actually used, the behavior of the models is most affected by the cooperating width of the reinforced concrete slab perpendicular to the direction of the horizontal force and the dimensions of the columns. We have shown that using the method of equivalent frames (linearly elastic) fitted to the results of nonlinear FE experiments, we can study the behavior of flat slabs with varying geometry.

For a given structural design, we have shown the accuracy of the method in the case of a five-stage approximation, thus showing that the method is suitable for modeling cases occurring in standard engineering practice. The practical applicability of the presented individual method can be achieved by extending the general geometry of the method, which is the goal of our research. By combining the results of the nonlinear numerical results with the much simpler but easier-to-use linearly flexible computational model, we have shown that a one- and two-variable function suitable for recording the replacement beam width can be generated. The results are illustrated in a 3D graph, which allows the reduction factor (β) for each grid ratio to be determined. By geometrically extending of the replacement beam width, in addition to completely unique geometrical parameters, the reduction factor (β) can be easily determined, with which the structure can be examined with a finite element software that can be used in everyday engineering practice. It should be noted that the results were determined from numerical studies and have specific geometrical constraints, however, these constraints are acceptable for high-rise structures.

In the case of one of the point-supported flat slabs models, we also operated horizontal cyclic loads of varying magnitude and direction, based on which the reduction factor (β_{cyc}) of the equivalent beam width can be determined for the case of cyclic tests. We also further supplemented the modeling technique we developed, based on which the value of the fixed crack coefficient (c_{fr}) can be taken to the following:

$$c_{fr} = 0.8 \,. \tag{6}$$

In cyclic studies, cyclic degradation was observed, but this only yielded significant results for larger deformations (horizontal displacement limits: 7 mm and 10 mm). At higher load levels, the cracking of the concrete elements is significant, and the degree of cyclic degradation can be quantified accordingly. With the applied crack propagation model, the rotating crack model is activated at lower load levels, and the fixed crack model is activated at higher load levels, so we get as close as possible to the real behavior.

Based on the results, it can be concluded that the improved modeling technique can be applied to study cyclical behavior. The equivalent beam width can be taken with a modification coefficient (r_{cyc}) determined from the cyclic tests. This modification coefficient can be used to determine the value of the reduction factor (β_{cyc}), in which it is already possible to take cyclic behavior into account (5). With the technique we have defined, the value of the reduction factor can be further extended to the geometry were tested in the research, so that the modification coefficient (r_{cyc}) and the reduction factor (β_{cyc}) for cyclic analyses can be generalized.

Overall, we have shown that the non-linear behavior of the structure can be taken into account in the linear elastic calculation, which was brought back to the linear elastic models based on the results of 3D non-linear finite element calculations, so in the case of the analysis of deformations in linear elastic models, we get results that are more in line with reality.

5 Further research opportunities

In the present research, we did not deal in detail with the reinforcement used in the column-slab models. In further research, we consider it necessary to examine these parameters as well. In any case, the results obtained by changing the reinforcements used in the column and in the slab can be forward-looking. Based on the results, the moment-rotation relationship at the connection between the column and the slab can be determined for each reinforcement quantity, which can also be applied in everyday engineering practice.

The effect of the design of the reinforcements was not taken into account in the present research either. The effect of the reinforcement was previously studied in the case of column-beam joints [5], and it was shown in our numerical studies that the alignment of the rebar has a significant effect on the load-bearing capacity and the deformability of the joint, so the efficiency of the reinforcement could be demonstrated with finite element software. Further testing for this is strongly recommended.

The present research program can be supplemented by considering additional parameters such as the length of the column. Furthermore, with the modeling technique we developed, more detailed studies can be performed by analyzing the stress and crack concentration at the connection of the column and the slab, and the bulging of the columns can also be examined.

Acknowledgement

We are grateful to the Department of Structural Engineering of the Budapest University of Technology and Economics for providing us with the applied software.

We thank to Pál Boldizsár Bodó, MSc for their technical assistance.

References

[1] Kim, K. S., Choi, S.-H., Ju, H., Lee, D. H., Lee, J.-Y., Shin, M. "Unified equivalent frame method for flat plate slab structures under combined gravity and lateral loads – Part 1: derivation", Earthquakes and Structures, 7(5), pp. 719–733, 2014. https://doi.org/10.12989/eas.2014.7.5.719

[2] Pecknold, D. A. "Slab Effective Width for Equivalent Frame Analysis", ACI Structural Journal, 72(4), pp. 135–137, 1975. https://doi.org/10.14359/11121

[3] Moehle, J. P., Diebold, J. W. "Lateral Load Response of Flat-Plate Frame", Journal of Structural Engineering, 111(10), pp. 2149–2164, 1985.

[4] Hwang, S., Moehle, J. P. "Models for Laterally Loaded Slab-Column Frames", ACI Structural Journal, 97(2), pp. 345–353, 2000.

[5] Haris, I., Roszevák, Z. "Finite element analysis of cast-in-situ RC frame corner joints under quasistatic and cyclic loading", Revista de la Construcción, 18(3), pp. 579–594, 2019. https://doi.org/10.7764/rdlc.18.3.579

[6] Farkas, G. "Magasépítési Vasbetonszerkezetek" (High-rise reinforced concrete structures), Műegyetemi Kiadó, 2007. (in Hungarian) ISBN:

[7] Bódi, I., Farkas, G. "Vasbeton lemezek" (Reinforced concrete slabs), Egyetemi segédlet v1.0, Budapest University of Technology and Economics, 2000. (in Hungarian) ISBN:

[8] Hwang, S. J., Moehle, J. P. "An Experimental Study of Flat-Plate Structures Under Vertical and Lateral Loads", Earthquake Engineering Research Center, University of California, Berkeley, CA, USA, Rep. UCB/EERC-93/03, 1993.

[9] Lapi, M., Isufi, B., Orlando, M., Ramos, A. "R/C Flat Slab-Column Connections Under Lateral Loading", presented at: ANIDIS 2017 – XVII Convegno ANIDIS "l'Ingegneria Sismica in Italia", Pistoia, Italy, Sep. 17–21, 2017.

[10] Vanderbilt, M. D., Corley, W. G. "Frame Analysis of Concrete Buildings", Concrete International, 5(12), pp. 33–43, 1983.

[11] Benavent-Climent, A., Zamora-Sánchez, D., Gil-Villaverde, J. F. "Experimental Study on the Effective Width of Flat Slab Structures under Dynamic Seismic Loading", Engineering Structures, 40, pp. 361–370, 2012. https://doi.org/10.1016/j.engstruct.2012.03.002

[12] Robertson, I. N. "Seismic Response of Connections in Indeterminate Flat-Slab Subassemblies", PhD Thesis, Rice University, 1990.

[13] Moehle, J. P. "Seismic Design and Performance Verification", McGraw-Hill Education, 2014. ISBN: 978-0-07-183945-7

[14] Zhou, Y, Hueste, M. D. "Review of Laborytory Test Data for Cimbined Lateral and Gravity Shear Demands On Interior Slab-Column Connections", presented at: 16th World Conference on Earthquake, 16WCEE, Santiago, Chile, Jan. 9–13, 2017.

[15] Haris, I., Roszevák, Z. "Előregyártott vasbeton gerendák numerikus és kísérleti vizsgálata" (Numerical and experimental investigation of prefabricated reinforced concrete beams), Vasbetonépítés, 19(1), pp. 2–11, 2017. (in Hungarian)

[16] Roszevák, Z., Bodó, P. B., Haris, I. "Vasbeton síklemez egyenértékű kerettel történő helyettesítése vízszintes teherre numerikus vizsgálatok alapján" (Replacement of a reinforced concrete slab with an equivalent frame for horizontal load based on numerical tests), presented at: XIII. Magyar Mechanikai Konferencia, Miskolc, Hungary, Aug. 27–29, 2019. (in Hungarian)

[17] Roszevák, Z., Haris, I. "Monolit vasbeton keretsarok és oszlop gerenda kapcsolatok numerikus és kísérleti vizsgálata" (Numerical and experimental investigation of monolithic reinforced concrete frame corner and column beam connections), XIII. Magyar Mechanikai Konferencia, Miskolc, Hungary, Aug. 27–29, 2019. (in Hungarian)

[18] Roszevák, Z., Haris, I. "Monolit vasbeton keretsarok numerikus vizsgálata - 1. rész Egyirányú monoton növekvő terhelés (Numerical investigation of monolithic reinforced concrete frame corner - Part 1 Unidirectional monotonically increasing load)" Vasbetonépítés, 21(3), pp. 78–86, 2019. (in Hungarian) https://doi.org/10.32969/VB.2019.3.3

[19] Roszevák, Z., Haris, I. "Monolit vasbeton keretsarok numerikus vizsgálata - 2. rész: Ciklikusan változó terhelés" (Numerical analysis of monolithic reinforced concrete frame corner - Part 2: Cyclically changing load), Vasbetonépítés, 22(3), pp. 74–82, 2020. (in Hungarian) https://doi.org/10.32969/VB.2020.3.2

[20] Roszevák, Z., Haris, I. "The effect of non-linear finite element analysis on the description of the global behavior of a prefabricated RC skeleton", International Journal Optimization in Civil Engineering, 11(3), pp. 515–546, 2021. [online] Available at: http://ijoce.iust.ac.ir/article-1-489-en.html

[21] Červenka, V. "Constitutive Model for Cracked Reinforced Concrete", ACI Journal, 82(6), 877–882, 1985. https://doi.org/10.14359/10409

[22] Darwin, D., Pecknold, D. A. W. "Inelastic Model for Cyclic Biaxial Loading of Reinforced Concrete", University of Kansas, Center for Research, Research Grant GI 29934, The National Science Foundation, 1974.

[23] Červenka, V., Jendele, L., Červenka, J. "ATENA Program Documentation Part 1, Theory", Cervenka Consulting Ltd, Prague, Czech Republic, 2014.

[24] Menegotto, M., Pinto, P.E. "Method of analysis of cyclically loaded RC plane frames including changes in geometry and non-elastic behavior of elements under normal force and bending", ABSE reports of the working commissions, 13, 1973. https://doi.org/10.5169/seals-13741

[25] fib "Model Code for Concrete Structures", International Federation for Structural Concrete, Lausanne, Switzerland, 2010. ISBN: 978-3-433-03061-5

[26] NZS "NZS 1170.5:2004, Structural Design Actions, Part 5, Earthquake Actions New Zealand", Standards New Zealand, Wellington, New Zealand, 2004.

[27] Government of Canada "NRCC.2005. National Building Code of Canada. Part 4: Structural design. Canadian Commission on Building and Fire Codes", National Research Council of Canada (NRCC), Ottawa, Canada, 2005.

[28] AS "AS1170.4 2007 Structural design actions, Part 4: Earthquake actions in Australia", Australian Standard, Sydney, Australia, 2007. [online] Available at: https://hdl.handle.net/2123/24025

[29] ICC "IBC-2009. International Building Code", International Code Council, Country Club Hills, IL, USA, 2009. [online] Available at: https://codes.iccsafe.org/content/IBC2009